

MR Imaging in the Evaluation of Cystic-appearing Soft-Tissue Masses of the Extremities¹

Ana Bermejo, MD • Teresa Díaz De Bustamante, MD • Alberto Martínez, MD
Roberto Carrera, MD • Elena Zabía, MD • Palmira Manjón, MD

SA-CME

See www.rsna.org/education/search/RG

LEARNING OBJECTIVES FOR TEST 5

After completing this journal-based SA-CME activity, participants will be able to:

- Distinguish between truly cystic (ie, fluid-filled) and solid cystic-appearing lesions.
- Discuss the spectrum of solid lesions that may have a cyst-like appearance at MR imaging.
- Describe specific imaging findings of a variety of solid benign and malignant myxoid tumors.

TEACHING POINTS

See last page

Cystic-appearing lesions are commonly seen in clinical practice at imaging of the extremities. However, only some of these lesions are truly cystic lesions (eg, ganglia or synovial cysts, bursae) and may be managed conservatively. Fluid-filled lesions usually have homogeneous high T2 signal at magnetic resonance (MR) imaging. A broad array of solid benign masses (eg, myxomas, peripheral nerve sheath tumors [PNSTs], certain vascular lesions, glomus tumors) and malignant solid masses (including undifferentiated pleomorphic sarcomas, myxofibrosarcomas, myxoid liposarcomas, synovial sarcomas, extraskeletal myxoid chondrosarcomas, and, less frequently, soft-tissue metastases) may also exhibit bright T2 signal at MR imaging, thereby simulating a cyst. On the other hand, fluid-filled lesions with associated complications (eg, bleeding or inflammatory changes) may have a more complex appearance. MR imaging plays a major role in distinguishing truly cystic lesions from solid lesions. If a cystic-appearing lesion demonstrates wall thickening or internal complexity (heterogeneous signal, nodules, or thick septa), evaluation with contrast material enhancement is mandatory, and a solid lesion must be suspected if any internal enhancement is present. In addition to categorizing the lesions as truly cystic or solid, the differential diagnosis may be further narrowed by considering the anatomic location of the lesion or characteristic imaging features (eg, internal linear or patchy enhancement at contrast-enhanced MR imaging and an intramuscular location in myxomas; the “split fat sign,” “string sign,” and “target sign” in PNSTs; tiny foci of fat in myxoid liposarcomas). In most cases, however, histologic analysis is required to achieve a definitive diagnosis.

©RSNA, 2013 • radiographics.rsna.org

Abbreviations: EIC = epidermal inclusion cyst, PNST = peripheral nerve sheath tumor, STIR = short inversion time inversion-recovery, UPS = undifferentiated pleomorphic sarcoma, WHO = World Health Organization

RadioGraphics 2013; 33:833–855 • Published online 10.1148/rg.333115062 • Content Codes: **MK** **MR** **OI**

¹From the Department of Radiology, Hospital Universitario Doce De Octubre. Avenida de Córdoba S/N, 28041 Madrid, Spain. Presented as an education exhibit at the 2010 RSNA Annual Meeting. Received March 28, 2011; revision requested June 28; final revision received January 21, 2013; accepted January 30. For this journal-based SA-CME activity, the authors, editor, and reviewers have no relevant relationships to disclose. **Address correspondence to A.B.** (e-mail: rudalies@gmail.com).

Introduction

At magnetic resonance (MR) imaging, fluid-filled masses are usually hypointense relative to muscle with T1-weighted sequences and highly hyperintense with T2-weighted or fluid-sensitive sequences due to the prolonged T2 relaxation time of water (1).

Besides truly cystic lesions such as ganglia or bursae, there are some solid masses that can also appear to be very T2 hyperintense. These lesions have been described as “cystlike” lesions by some authors (2) and can simulate the T2 hyperintensity of truly cystic lesions by virtue of their high intratumoral water content (1,2). Ma et al (2) related the cystic appearance of solid masses to the presence of internal necrosis, high extracellular water content (edema around the nonnecrotic cells), or an extracellular matrix with high water and protein content (myxoid stroma). Myxoid material consists of a gelatinous matrix stroma with high levels of hyaluronic acid and immature collagen fibers. Because of its high water content, myxoid material appears hyperintense on T2-weighted MR images (1). It may be present in benign tumors such as myxoma, and in malignant soft-tissue tumors such as myxoid liposarcoma, myxoid chondrosarcoma, and myxoid malignant fibrous histiocytoma (3)—now referred to as undifferentiated pleomorphic sarcoma (4)—accounting for the cystlike appearance of these tumors. Other tissues that can mimic fluid on T2-weighted MR images include hyperemic synovium and hyaline cartilage (1).

These solid lesions can be mistaken for fluid-filled structures, which poses a diagnostic dilemma because of the relatively homogeneous hyperintensity seen in some of these lesions. MR imaging has proved useful for distinguishing cystic from solid lesions and allows a specific diagnosis to be made for certain lesions. It is important to attempt to make a distinction between benign and malignant masses in this category, since there are important implications for further management, such as the requirement for needle biopsy as opposed to excision biopsy or conservative management.

For didactic purposes, lesions with a cystic MR imaging appearance may be classified into

one of the following general diagnostic categories: truly cystic (benign) lesions, benign cystlike solid or partly solid lesions, and malignant (and intermediate-grade) solid lesions (Table 1).

In this article, we review various types of fluid-filled and cystlike solid lesions in terms of imaging approach and the MR imaging features of the most common lesions in each of the aforementioned categories.

Imaging Approach

Ultrasonography

Ultrasonography (US) (both gray-scale and Doppler) may be the initial imaging modality of choice for palpable soft-tissue masses due to its low cost and wide availability. Soft-tissue lesions can be categorized as cystic or solid depending on their echogenicity. At US, simple cysts are typically well defined and anechoic, with deep acoustic enhancement. Other fluid-containing lesions such as abscesses and hematomas have a different appearance, with low-signal-intensity internal echoes that may be homogeneous or heterogeneous. These lesions do not show deep enhancement, and they may have thick or irregular walls (5). A soft-tissue lesion must be suspected in the absence of anechoic content or deep enhancement, or if internal vascularization is depicted at Doppler US. Soft-tissue masses that are identified but not characterized with US require further investigation, usually with MR imaging. MR imaging is also superior in demonstrating the relationship between the mass and neighboring structures.

Computed Tomography

Although the utility of computed tomography (CT) in evaluating soft-tissue lesions is limited, fluid-filled lesions may be incidentally noted as low-attenuation masses at routine CT performed for some other reason.

MR Imaging

Because of its excellent tissue contrast, multiplanar capability, and lack of ionizing radiation, MR imaging has become the modality of choice in the evaluation of soft-tissue masses. Its potential to help discriminate between solid and cystic lesions has been well demonstrated.

Teaching
Point

RadioGraphics

Table 1
Lesions with a Cystic MR Imaging Appearance

Category	Types of Lesions	Patient Age	Anatomic Location
Truly cystic (benign) lesions	Synovial or ganglion cysts	All ages	Related to joints or tendons
	Distended bursae	All ages	Various locations
	Postsurgical collections and hematomas	All ages	Postsurgical locations, contusion sites
	Skin appendage lesions	Adults	Superficial
	Lymphatic malformations	Children (most commonly)	Common in head and neck, uncommon in extremities
Benign cystlike solid or partly solid lesions	Hydatid cysts	Adults (in endemic areas)	Rare in soft tissues
	Myxomas	Young to middle-aged adults	Frequently intramuscular
	PNSTs	Young adults	Extending along nerve roots (superficial or deep)
	Vascular lesions (hemangiomas and vascular malformations)	Children, adults	Sometimes intramuscular
Malignant (and intermediate-grade) solid lesions	Glomus tumors	Young to middle-aged adults	Digits
	UPS	Most common sarcoma in patients >50 y	Intramuscular or deep seated
	Myxoid sarcomas		
	Myxofibrosarcoma	Elderly	Lower limbs (superficial)
	Myxoid liposarcoma	Young adults	Thigh (deep seated)
	Extraskeletal myxoid chondrosarcoma	Middle-aged adults	Proximal extremities (deep) with extracompartmental invasion
Synovial sarcoma	Adolescents, young adults	Extremities near joints (common in popliteal fossa)	
Metastases	Adults	Superficial or deep, very rare	

Note.—Tumors categorized according to the World Health Organization (WHO) classification system established in 2002. PNST = peripheral nerve sheath tumor, UPS = undifferentiated pleomorphic sarcoma.

Imaging Strategy.—With imaging of soft-tissue masses, the lesion should be demarcated prior to imaging, but care should be taken not to compress or distort the mass. The selection of coils and imaging planes depends on the size and location of the mass. Surface coils adapted to the specific anatomic area must be used in each case, choosing the smallest coil that covers the entire lesion.

Initially, the use of a large field of view that includes the contralateral side should be considered to establish the presence of a soft-tissue mass. This approach is particularly applicable in the thighs, calves, and, occasionally, the upper thorax and shoulder girdle (1). A smaller field of view targeted to the lesion is indicated for detailed assessment of the mass and surrounding structures.

Imaging Sequences.—Images should be acquired in at least two perpendicular planes. Pulse sequences should include T1- and T2-weighted spin-echo sequences, the latter performed both with and without fat saturation. The use of fat suppression is particularly useful in the evaluation of subcutaneous masses. However, T2-weighted or even proton-density-weighted sequences without fat saturation provide good anatomic detail and tumor-to-muscle contrast. A short inversion time inversion-recovery (STIR) sequence may be added to or replace the fat-suppressed T2-weighted sequence because it can allow more homogeneous fat suppression, although

it has a lower signal-to-noise ratio and is more susceptible to degradation by motion (6).

Systems with higher field strength (typically 3.0 T) are now available in clinical practice. They provide a high intrinsic signal-to-noise ratio, potentially higher resolution (spatial and temporal), and improved contrast. A 3.0-T system may permit fast routine imaging or higher-resolution studies. Faster imaging will result in less patient motion, increased patient comfort, and better throughput. Increased resolution may result in more accurate diagnosis, but this assessment will require prospective validation (7).

Use of Intravenously Administered Gadolinium-based Contrast Agents.

—Strict evaluation of the MR imaging characteristics of these lesions is fundamental. A purely cystic mass usually shows homogeneous low signal intensity (lower than that of muscle) on T1-weighted images and homogeneous high signal intensity (similar to that of fluid) on T2-weighted images. Some fluid-filled lesions also arise in typical locations such as the periarticular soft tissues, the anatomic bursae, or a postsurgical area. Although location can be used to favor a given diagnosis, other lesions must be considered if the imaging findings are indeterminate.

Evaluation with contrast material enhancement is indicated when a cystic-appearing lesion (a) is identified in an atypical location, or (b) has heterogeneous internal signal, a thick wall, multiple or thick septa, or solid components, findings that suggest that the lesion is not a simple cyst (2).

In most cases, contrast-enhanced fat-saturated T1-weighted images obtained in two or three planes are sufficient for detecting solid enhancement. Alternatively, dynamic contrast-enhanced rapid gradient-echo T1-weighted imaging can be used.

When a lesion has high signal intensity with the spin-echo T1-weighted sequence, precontrast fat-suppressed T1-weighted imaging is helpful in establishing a baseline before the intravenous administration of gadolinium-based contrast material. Fat-suppressed T1-weighted imaging also aids in differentiating (a) fat from melanin or methemoglobin, and (b) fibrous or hemosiderotic parts from highly cellular components in tumors (8). Baseline acquisition is useful for obtaining subtraction images, which help detect subtle solid

enhancement. Images obtained before and after contrast administration must be obtained with identical imaging parameters to allow adequate assessment of enhancement.

An important consideration is that, given sufficient time, cystic structures (as well as joint fluid) may demonstrate gadolinium absorption and redistribution in the extracellular space, thereby mimicking solid enhancement. Although this enhancement is considerably less than that of a solid lesion, it can be artificially increased by the addition of fat suppression. Because this is a time-dependent phenomenon, patients should be imaged as soon as possible after gadolinium administration (9).

Four patterns of enhancement have been described: no enhancement, minimal thin rim enhancement (unilocular or multilocular), thick rim enhancement, and solid enhancement (2). If a T2-hyperintense mass has a thin rim of peripheral enhancement and no internal enhancement, it is a truly cystic (ie, fluid-filled) lesion. Ganglia are very common and should be considered whenever a periarticular mass with these characteristics is identified at MR imaging (Fig 1). Other lesions that may demonstrate a thin rim of peripheral enhancement include postoperative seromas, lymphoceles, epidermal inclusion cysts (EICs), and lymphangiomas (1).

Other diagnoses must be considered when the peripheral rim of enhancement is thick or irregular, including inflamed or infected ganglia, abscesses, hematomas, and necrotic tumor masses (2,10).

If a T2-hyperintense mass demonstrates some degree of internal enhancement, soft-tissue masses (eg, intramuscular myxomas, myxoid sarcomas, PNSTs, synovial sarcomas) should be considered (1).

Therefore, if solid enhancement or thick rim enhancement is present, a histologic specimen should be obtained to rule out a malignant lesion.

Fast dynamic contrast-enhanced gradient-echo T1-weighted imaging has proved useful in determining tumor viability and can, therefore, be helpful in selecting a biopsy site, assessing therapy response, and evaluating for the presence of local recurrence in patients with soft-tissue sarcomas (11). Contrast enhancement may also be helpful in highlighting tissue planes to aid in assessing the degree of invasion of a mass into vessels and other structures. It can also play an important role in helping to target tumor nodules in cystic or hemorrhagic masses during biopsy (12).

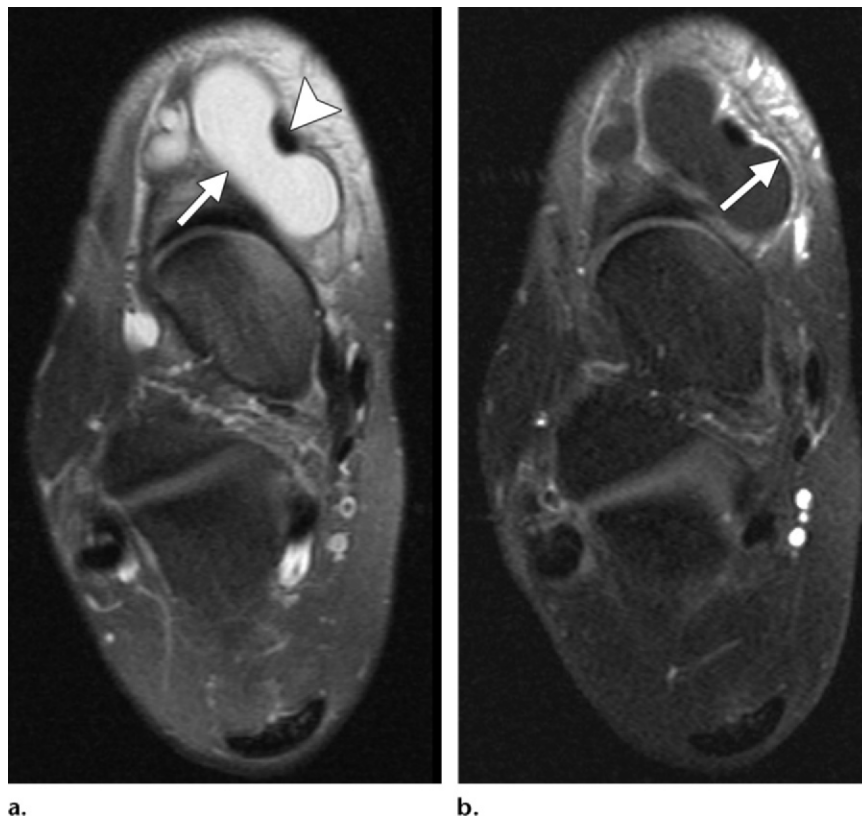


Figure 1. Ganglion cyst in a 47-year-old patient with a history of a palpable mass in the right ankle. **(a)** Long-axis fat-suppressed T2-weighted MR image shows a well-defined lesion with a lobular contour and a thin lining (arrow) in close relationship to the anterior tibial tendon (arrowhead). The lesion demonstrates homogeneous high signal intensity compatible with that of fluid. **(b)** On a long-axis contrast-enhanced fat-suppressed T1-weighted MR image, the lesion demonstrates thin rim enhancement (arrow) with no internal or nodular enhancement, findings that confirm its cystic nature.

MR imaging plays a major role in distinguishing benign from malignant lesions. In an effort to make this distinction, Harish et al (13) suggested that the MR imaging features most suggestive of malignant lesions included greater average size (>7 cm), larger maximum dimension (>10 cm), and heterogeneity on T1-weighted MR images. Malignant lesions tend to show more intense and more rapid enhancement (14). However, enhancement cannot reliably help distinguish benign from malignant lesions (12,14), since there is an overlap of the imaging characteristics of malignant and highly vascularized benign lesions. It has been shown that the addition of dynamic contrast-enhanced imaging may improve the differentiation between benign and malignant soft-tissue masses (15,16). It has also been postulated that perfusion-corrected diffusion-weighted MR imaging may play a role in this differentiation by showing significantly increased true diffusion in benign masses compared with malignant lesions (17). However, because the imaging characteristics of benign and malignant soft-tissue masses may overlap, histologic analysis may be necessary to achieve a definitive diagnosis.

Truly Cystic Lesions

Ganglia and Synovial Cysts

Synovial cysts are a result of herniation of the synovial membrane through the joint capsule.

Ganglion cysts have no synovial lining. They have a fibrous lining, contain fluid or mucinous material, and arise from the joint capsule, ligaments, tendon sheaths, bursae, or subchondral bone (18). Ganglia are usually found in the periarticular soft tissues in areas under repetitive stress (eg, the dorsum of the wrist) and may or may not show communication with joint spaces. Sometimes, they can occur far away from a joint or even in an intramuscular location.

In clinical practice, the terms *ganglion cyst* and *synovial cyst* are frequently used interchangeably due to the common periarticular location of these lesions and the fact, in most cases, radiologic differentiation is not possible.

At MR imaging, uncomplicated synovial and ganglion cysts demonstrate a thin rim and may

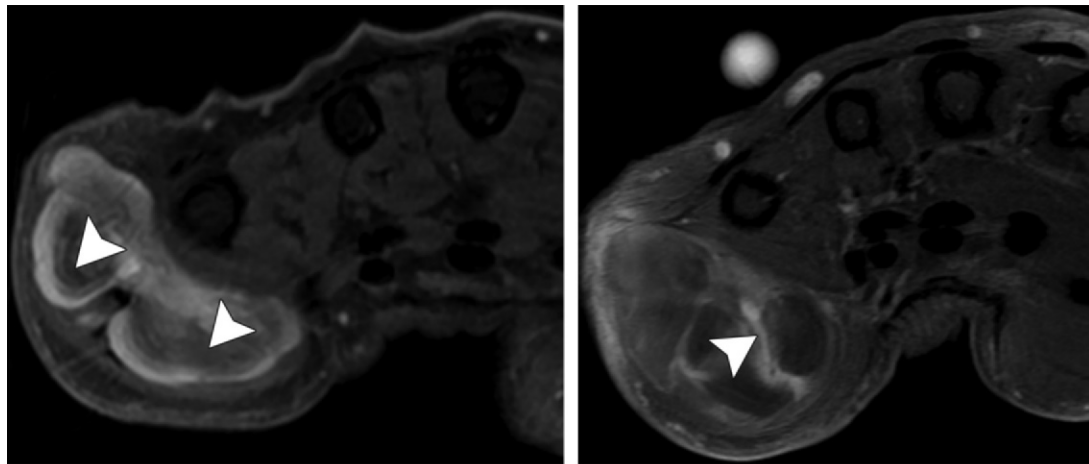


Figure 2. Bleeding within a ganglion cyst in a 90-year-old woman who presented with mass effect in the left hypothalar eminence. **(a)** Axial fat-suppressed T2-weighted MR image shows a high-signal-intensity lobulated mass with hypointense content (arrowheads), likely related to early subacute bleeding. Hyperintense foci were noted within the mass on T1-weighted images. **(b)** Contrast-enhanced fat-suppressed T1-weighted MR image shows the mass with a thick rim and septal enhancement (arrowhead), but no central enhancement or solid components.

have thin internal septa, both of which may enhance after gadolinium administration, with a lack of central enhancement otherwise (Fig 1) (2).

Ganglia may be associated with a track extending toward the joint and may demonstrate pericyclic edema (19). They may have high signal intensity (higher than that of muscle) on T1-weighted images, reflecting higher proteinaceous or hemorrhagic content. Also, typical ganglia usually demonstrate homogeneous high signal intensity on T2-weighted images, but they may have a more heterogeneous appearance.

A complication (bleeding or inflammatory changes) may also be present. Complicated synovial and ganglion cysts may have a more heterogeneous appearance with low or bright internal signal intensity, depending on the evolution of bleeding. There may also be thickening of the outer lining or internal septa in cases of infectious or inflammatory changes. However, they should not demonstrate internal enhancement after intravenous contrast administration (Fig 2).

Bursae

Bursae are synovium-lined virtual spaces in areas of increased friction that may or may not be connected to joint spaces. Bursae are often incidentally found in typical locations such as the popliteal fossa. Popliteal cysts (also known as Baker cysts) are lined with synovium and result from the extrusion of joint fluid into the gastrocnemius-



Figure 3. Baker cyst. Axial fat-suppressed T2-weighted MR image of the left knee shows a posteromedial cyst (arrow) that extends between the medial head of the gastrocnemius muscle (white arrowhead) and the semimembranosus tendon (black arrowhead).

semimembranosus bursa through a weak portion of the posteromedial capsule of the knee between the medial head of the gastrocnemius muscle and the semimembranosus tendon (Fig 3) (18). Other common bursae in well-known anatomic locations include the prepatellar bursa (located between the patella and the overlying subcutane-

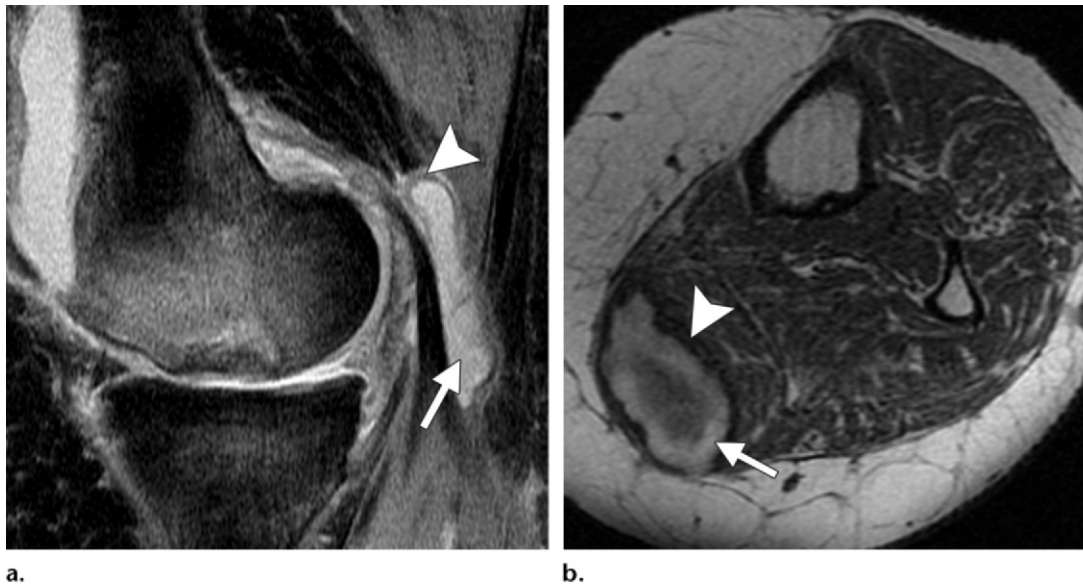


Figure 4. Bleeding within a Baker cyst in a 74-year-old patient with a subchondral insufficiency fracture of the left medial femoral condyle. **(a)** Sagittal fat-suppressed T2-weighted MR image shows a Baker cyst (arrow) with wall thickening (arrowhead). The cyst was dissecting through the inner aspect of the medial gastrocnemius muscle as a result of rupture. **(b)** Axial T1-weighted MR image shows a subacute hematoma with peripheral high signal intensity (arrow) and a low-signal-intensity rim (arrowhead).

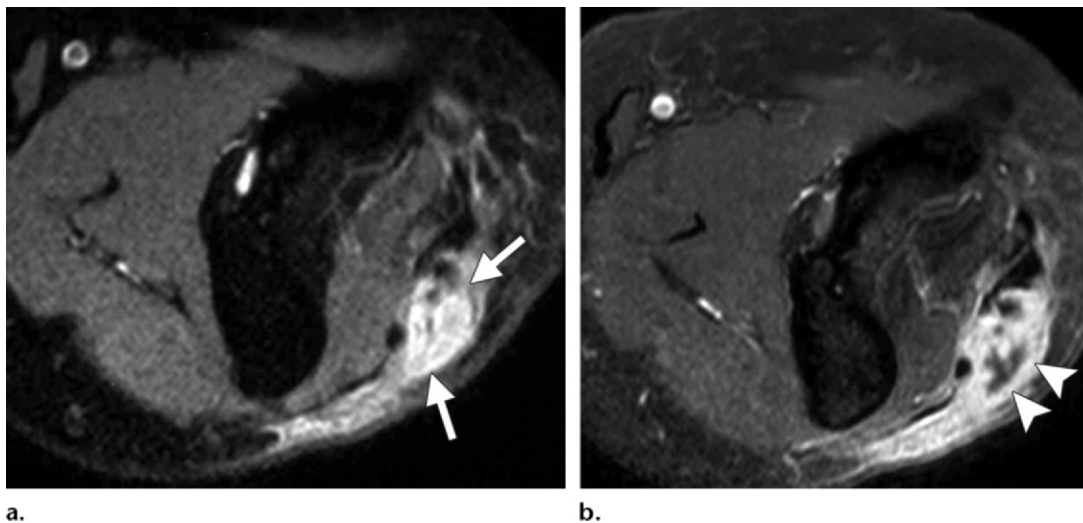
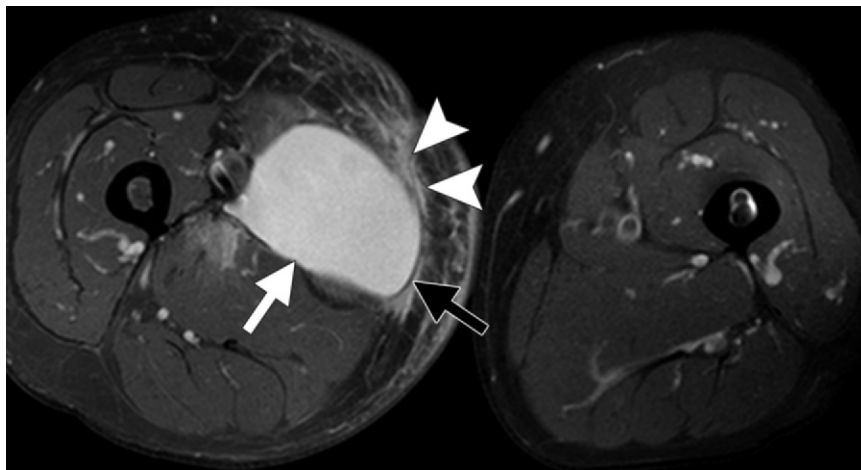


Figure 5. Olecranon bursitis in a 32-year-old woman with disseminated tuberculosis. **(a)** Axial fat-suppressed T2-weighted MR image shows a cystic-appearing lesion in the expected location of the left olecranon bursa (arrows) with adjacent soft-tissue edema. **(b)** On an axial contrast-enhanced fat-suppressed T1-weighted MR image, the lesion demonstrates thick rim enhancement (arrowheads). Osseous extension (not shown) was also present. Acid-fast bacilli culture of the synovial fluid revealed mycobacterial growth.

ous tissues), anserine bursa (located between the pes anserinus tendons and the subjacent distal portion of the tibial collateral ligament), iliopsoas and bicipital bursae (which follow the iliopsoas and biceps tendons, respectively, to their distal attachment), and olecranon bursa (located over the extensor aspect of the extreme proximal end of the ulna).

A bursa may appear heterogeneous because of the presence of internal loose bodies or synovial debris. Signs of complications may also be present due to bleeding (Fig 4) or inflammatory changes (bursitis) (Fig 5), which may result in wall thickening (thick rim) and heterogeneous

Figure 6. Seroma following surgery for a liposarcoma of the right thigh in a 79-year-old man. Axial fat-suppressed T2-weighted MR image shows an enlarged right thigh with marked asymmetry. A well-defined, homogeneously hyperintense deep collection (white arrow) surrounded by a thin capsule (black arrow) is present in the surgical area. Adjacent subcutaneous edema is also present (arrowheads).



fluid accumulation. In these cases, contrast administration may be necessary to exclude solid components.

Postsurgical Collections and Hematomas

Abscesses and, to a lesser extent, lymphoceles and seromas may appear at MR imaging as complex cystic lesions with a thick rim and heterogeneous signal intensity on T1-weighted images. They usually demonstrate high T2 signal (Fig 6); however, this signal is usually not as homogeneous as that of ganglia or cysts. Adjacent soft-tissue inflammation is an associated finding that may help support a diagnosis of abscess.

Even in a postsurgical setting, contrast administration is often necessary to exclude solid lesions (especially sarcomas with a necrotic center). Postsurgical collections usually have thin or unilocular thick rim enhancement without central enhancement.

The appearance of hematomas at MR imaging is highly variable and time dependent. Hyperacute blood (within 24 hours) is rarely imaged, but it has intermediate signal intensity (similar to that of muscle) on T1-weighted images and high signal intensity on T2-weighted images. In the acute stage (1–3 days), hematomas have intermediate signal intensity on T1-weighted images and intermediate to low signal intensity on T2-weighted images due to the high concentration of intracellular deoxyhemoglobin. Early subacute hematomas (>3 days) are hyperintense on T1-weighted images (similar to fat)

due to intracellular accumulation of methemoglobin, and hypointense on T2-weighted images. Older subacute hematomas (>7 days) have high signal intensity on both T1- and T2-weighted images due to the presence of extracellular methemoglobin. With both T1- and T2-weighted sequences, chronic hematomas (>14 days) may demonstrate a hypointense center and a low-signal-intensity rim due to fibrosis and hemosiderin deposition (Fig 4) (20,21).

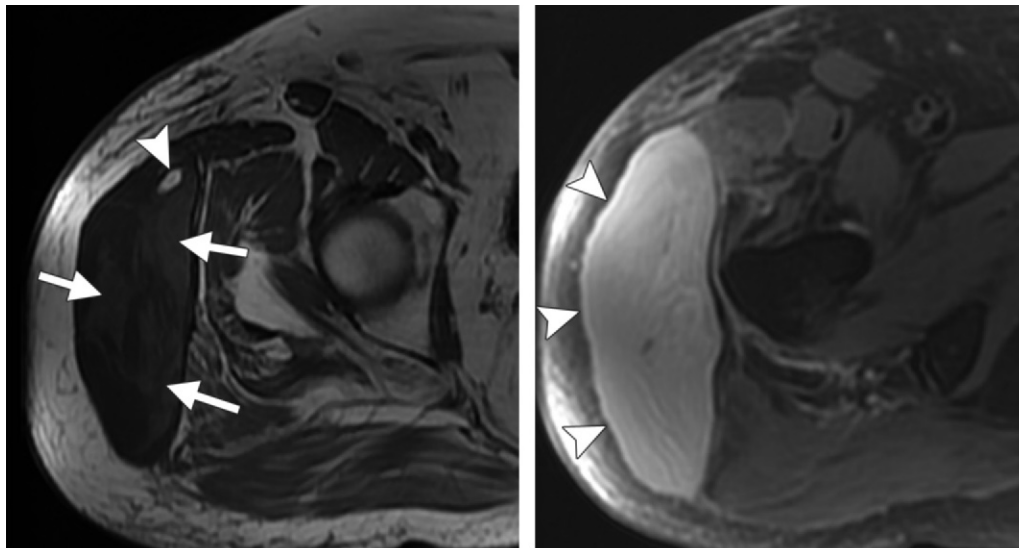
A hematoma in an intramuscular location may appear more heterogeneous due to repeated bleeding from muscle contraction. It is sometimes difficult to distinguish between a posttraumatic hematoma and a hematoma due to bleeding within a soft-tissue tumor; thus, special care must be taken to exclude any solid-appearing component within the hematoma (20).

Morel-Lavallée lesions must be considered as a separate entity due to their distinctive imaging features. They represent closed degloving post-traumatic injuries, generally manifest as a hemolymphatic mass, and are commonly located over the external aspect of the thigh or anteriorly in the knee in a perifascial location. Their MR imaging characteristics depend on the concentration of hemolymphatic fluid, the chronicity of blood products, and the presence of fat globules (Fig 7) (22).

In all of the aforementioned lesions, a history of surgery, sepsis, or trauma may suggest the diagnosis.

Skin Appendage Lesions

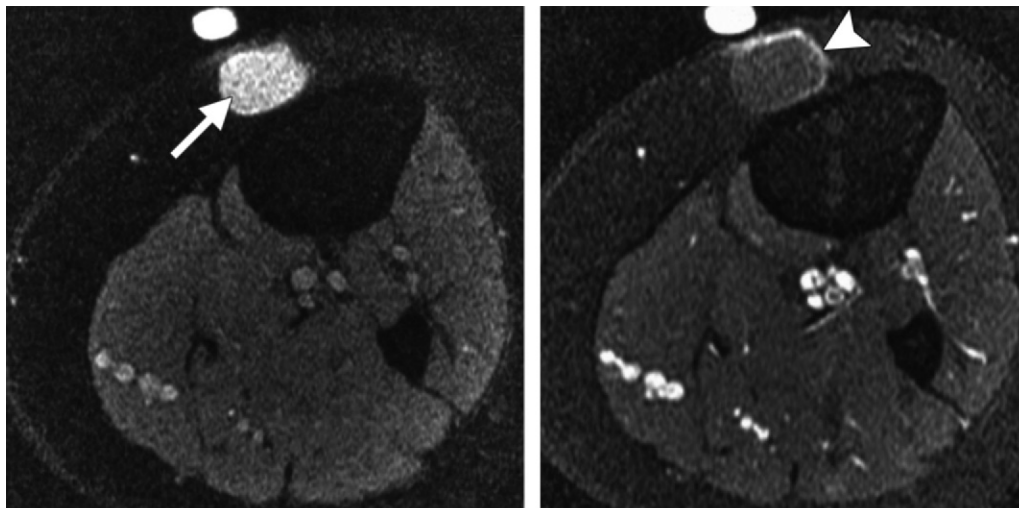
Skin appendage lesions originate in the epidermis and dermis. EICs (or infundibular cysts) are probably the most common of these le-



a.

b.

Figure 7. Morel-Lavallée lesion in a 60-year-old patient with previous pelvic trauma. **(a)** Axial T1-weighted MR image reveals a well-circumscribed subcutaneous collection with intermediate signal intensity (arrows) due to the presence of subacute blood. The collection is located superficial to the right tensor fascia lata and contains a globule of fat (arrowhead). **(b)** On an axial fat-suppressed T2-weighted MR image, the collection demonstrates high signal intensity (arrowheads).



a.

b.

Figure 8. EIC in a 28-year-old woman. **(a)** Axial fat-suppressed T2-weighted MR image shows a well-defined, hyperintense subcutaneous mass (arrow) anterior to the left tibial diaphysis. The mass demonstrated homogeneous low signal intensity on T1-weighted images. **(b)** Axial contrast-enhanced fat-suppressed T1-weighted MR image shows the mass with only minimal thin rim enhancement (arrowhead).

sions. EICs are subcutaneous cysts filled with keratin debris and lined by a wall of stratified squamous epithelium. Fewer than 10% occur in the extremities. These lesions are usually diagnosed clinically, but sometimes they are seen

incidentally at MR imaging, having a truly cystic appearance (Fig 8). However, EICs may demonstrate high signal intensity due to proteinaceous

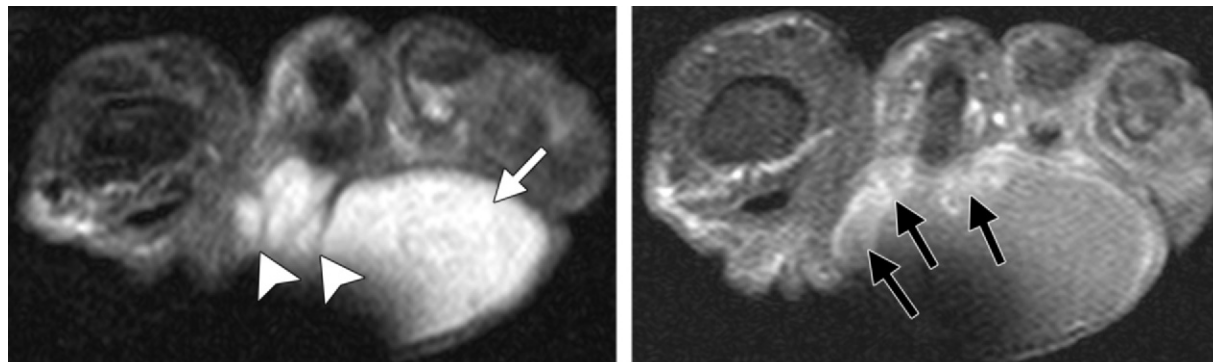


Figure 9. Ruptured EIC on the plantar surface of the left foot in a 63-year-old woman. **(a)** Axial fat-suppressed T2-weighted MR image shows a well-defined, high-signal-intensity subcutaneous lesion (arrow). The homogeneous increased signal intensity suggests a possible cystic mass. Note the thin, hypointense internal septa (arrowheads). **(b)** Axial gadolinium-enhanced fat-suppressed T1-weighted MR image shows the lesion with irregular thick rim enhancement (arrows). Subtle enhancement of adjacent subcutaneous tissue (not shown) was also evident. Postexcision histologic analysis revealed a ruptured EIC.

content on T1-weighted images, or components with variable low signal intensity on T2-weighted images. After contrast administration, they demonstrate peripheral thin rim enhancement with lack of central enhancement (23).

Ruptured EICs demonstrate thick and irregular peripheral rim enhancement (Fig 9), surrounding soft-tissue reactions, and variable septa, simulating infectious or neoplastic lesions at MR imaging, and histologic analysis may be necessary (23).

Lymphatic Malformations

Although lymphatic malformations are commonly known as cystic hygromas or lymphangiomas, *lymphatic malformations* is the currently preferred term, since the suffix “-oma” should be reserved for lesions that exhibit cellular proliferation (24). These slow-flow lesions occur most often in the pediatric population and seldom in the extremities. Although they may involve almost every organ system, soft-tissue lymphatic malformations most commonly occur in cervicofacial (up to 75% of cases), axillary (up to 25%), or mediastinal (3%–10%) areas (25). Lymphatic malformations may be mixed with other vascular malformations (6). Depending on the size of the cystic components, lymphatic malformations may be microcystic or macrocystic (in which case they are often referred to as cystic hygromas). These fluid-containing spaces correspond to the histologic findings of ectatic lymphatic channels.

At MR imaging, lymphatic malformations appear as multiseptated cystic masses that can infil-

trate surrounding tissues, sometimes causing hypertrophy of the affected body part. The cysts are typically hypointense on T1-weighted images and hyperintense on T2-weighted images. More heterogeneous signal intensity may be seen within cysts with proteinaceous or hemorrhagic content. The cysts do not characteristically enhance, although the septa, which are vascularized, show contrast material uptake. There may also be enhancement of the venous component in mixed malformations. In the microcystic form, the cysts may not be visible as distinct elements, and the lesion may appear slightly hyperintense after gadolinium administration due to septal enhancement (6).

Hydatid Cysts

Hydatid disease is the most common disease caused by helminths (larval forms of small *Echinococcus granulosus* tapeworms) in humans (26). Musculoskeletal involvement is seen in only 1%–4% of cases, usually in association with skeletal lesions (27), without concomitant hepatic or pulmonary involvement. Several patterns of disease have been recognized using various imaging techniques. These patterns include the unilocular cyst, multilocular lesion, and atypical complex or solid lesion. A multilocular lesion with several daughter cysts inside the mother cyst is characteristic of, but not pathognomonic for, hydatid disease. On T1-weighted MR images, the signal intensity pattern of the daughter cysts reflects their contents and may vary according to whether the parasites are dead or alive (26). On T2-weighted images, the cystic lesions usually have high signal intensity (Fig 10). The presence of a bacterial infection or

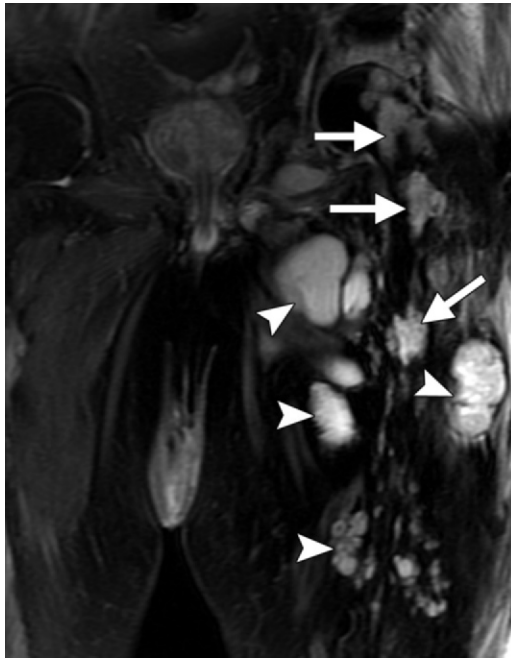


Figure 10. Musculoskeletal hydatidosis in a 79-year-old man who had previously undergone surgery for hydatidosis. Coronal T2-weighted STIR MR image demonstrates numerous soft-tissue and intramuscular cystic lesions (arrowheads) and hyperintense osseous lesions (arrows) in the proximal left thigh.

abundant intracystic debris and inflammatory changes may affect the typical morphologic features of a cyst, transforming it into a complex or solid lesion mimicking a tumor (26).

Hydatid cysts must be suspected in endemic areas. In these rare cases, the patient's history and clinical examination results are extremely helpful in reaching the correct diagnosis. Contrast administration may be necessary, with significant peripheral enhancement usually being seen afterward.

Benign Cystlike Solid or Partly Solid Lesions

We have categorized benign soft-tissue lesions according to the WHO classification system established in 2002 (Table 1) (4). We have also added other neoplasms such as vascular malformations and glomus tumors, lesions that are not part of the WHO classification system but that may manifest with a cystic appearance.

Myxomas

The term *myxoma* was introduced by Virchow in 1863 to designate a tumor that histologically resembled the umbilical cord. Stout established initial criteria for the diagnosis of myxoma in 1948, namely, a true mesenchymal neoplasm composed of undifferentiated stellate cells in a myxoid stroma. Myxomas frequently arise in an intramuscular location (up to 82% of cases in some series) (28) and are seen less frequently in an intermuscular or subfascial location. They are

generally seen in young to middle-aged patients and have a slight female predilection. The association between intramuscular myxoma and fibrous dysplasia is known as Mazabraud syndrome.

Typically, intramuscular myxomas are well-defined ovoid lesions with homogeneous fluid-like signal intensity on T2-weighted images (29). This appearance is a direct reflection of the high mucin and low collagen content within the lesion and represents a large amount of water. Contrast-enhanced imaging more accurately reflects the truly solid (although usually hypocellular) consistency of the myxoma, which demonstrates internal enhancement (28).

Three patterns of enhancement have been described after contrast administration: (a) peripheral enhancement with no internal enhancement due to the presence of a pseudocapsule, (b) peripheral and internal enhancement with linear stranding inside the tumor, and (c) peripheral enhancement with central areas of focal patchy or heterogeneous enhancement (Fig 11) (30).

The presence of more prominent enhancement has been related to tumors with more cells and less myxoid tissue (30), but also to focal areas of relative hypervascularity (29). Cystic components are frequently identified at contrast-enhanced MR imaging and pathologic examination (28).

The presence of a thin, perilesional fat rind on T1-weighted images has been described in up to

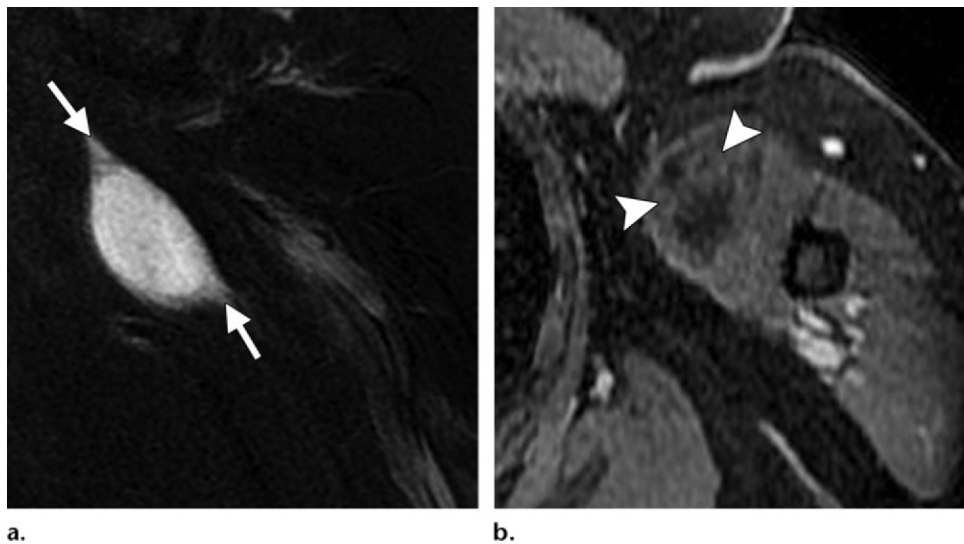


Figure 11. Myxoma in a 64-year-old woman. **(a)** Coronal STIR MR image of the left upper arm shows a well-defined, high-signal-intensity mass arising within the biceps brachii muscle, with a small amount of perilesional edema (arrows). **(b)** Axial gadolinium-enhanced fat-suppressed T1-weighted MR image shows the mass (arrowheads) with subtle peripheral and heterogeneous internal enhancement.

70% of cases and has been related pathologically to fatty muscle atrophy (28). On T2-weighted images, myxomas may have fine linear stranding representing thin fibrous septa within the tumor (30).

Perilesional edema with fluid-sensitive MR imaging sequences has also been described as suggestive of intramuscular myxoma (29). In addition, however, such edema has been described in other benign (eg, ganglia) and malignant (eg, UPS, myxoid sarcomas [myxofibrosarcoma, myxoid liposarcoma, extraskeletal myxoid chondrosarcoma]) lesions that can also occur in an intramuscular location (13). Therefore, perilesional edema is considered a nonspecific finding.

Cystic lesions may mimic the appearance of intramuscular myxoma on unenhanced MR images, but such lesions do not typically have an intramuscular location and represent true nonenhancing cystic lesions.

Intramuscular myxoma must also be differentiated from other deep myxoid lesions located in the extremities, including myxoid PNSTs, myxofibrosarcoma, myxoid liposarcoma, extraskeletal myxoid chondrosarcoma, and UPS. These lesions

are described in the sections that follow.

Even with cytopathologic analysis performed with fine-needle aspiration, benign myxomas can sometimes be misdiagnosed as myxoid malignancies and vice versa (30). Therefore, core-needle biopsy or even surgical biopsy may be necessary for definitive diagnosis.

Peripheral Nerve Sheath Tumors

PNSTs are classified separately as neurogenic tumors by the WHO and include benign and malignant PNSTs (1). Benign PNSTs and 10% of malignant PNSTs may have a large myxoid component (30).

Benign PNSTs include both schwannomas (neurilemmomas) and neurofibromas, which together account for 10% of benign soft-tissue tumors (31). They most commonly affect patients 20–30 years of age and have no gender predilection (32).

Schwannomas commonly occur along the spinal and sympathetic nerve roots of the head and neck and along the nerves in the flexor aspects of the upper and lower limbs (particularly the ulnar

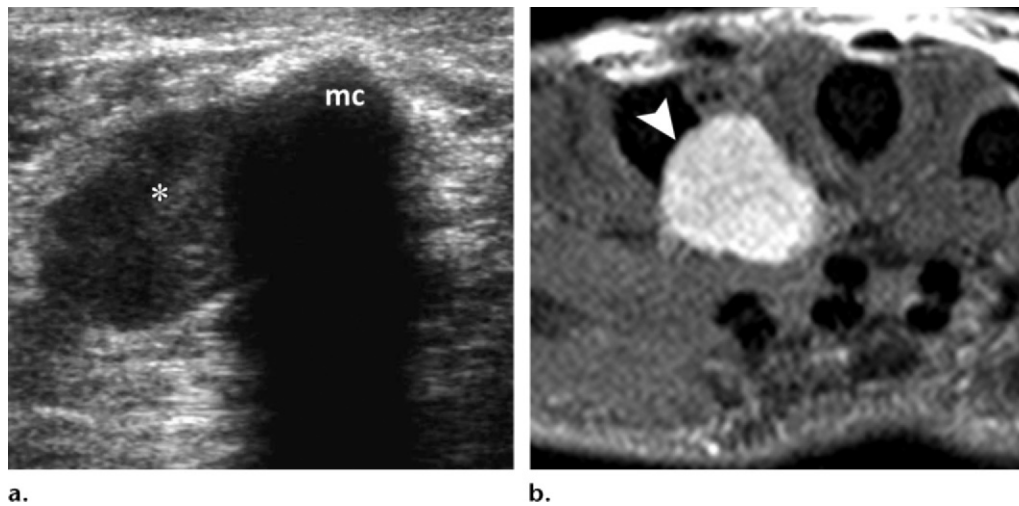


Figure 12. Schwannoma in a 78-year-old patient with a history of a tender palpable mass in the right hand. **(a)** US image shows a nodular hypoechoic mass (*) adjacent to the cubital margin of the second metacarpal bone (*mc*). **(b)** Axial fat-suppressed T2-weighted MR image shows an ovoid high-signal-intensity mass. Note the bone remodeling (arrowhead), a finding that is suggestive of a slow-growing lesion.

and peroneal nerves). The posterior mediastinum and retroperitoneum may also be affected (32).

Neurofibromas are found in the setting of neurofibromatosis in up to 10% of cases. This comorbidity results in a markedly increased risk of malignant transformation (33). Musculoskeletal abnormalities predominate in neurofibromatosis type 1, the most common form, as opposed to central nervous system manifestations in neurofibromatosis type 2. Neurofibroma classically comprises three subtypes: localized (arising from cutaneous or, occasionally, deeper-seated nerves), diffuse (originating from subcutaneous nerves in the head and neck), and plexiform (diffuse tumor extending along the branches of a nerve). Localized neurofibromas usually manifest as fusiform masses, similar to schwannomas (32,33). Consequently, it can be difficult to distinguish between schwannomas and neurofibromas at imaging.

Schwannomas tend to be encapsulated, eccentric to the nerve, and excisable from the nerve. Nonencapsulated neurofibromas are intermixed with and inseparable from nerve fibers (32). At MR imaging, schwannomas and nonencapsulated neurofibromas have a similar appearance, being nonspecific le-

sions that are hypointense relative to muscle on T1-weighted images and slightly hyperintense relative to fat on T2-weighted images (Fig 12). Enhancement on contrast-enhanced MR images may vary. However, the following signs have been described as characteristic at MR imaging (32).

1. The “split fat sign,” in which the lesion is surrounded by a rim of fat (Fig 13a). This finding is likely related to displacement of the fat that normally surrounds the neurovascular bundle.

2. The “string sign,” in which entering and exiting nerve roots are visualized at both ends of a vertically oriented fusiform mass (Fig 13b).

3. The “target sign,” in which the lesion demonstrates a high-signal-intensity peripheral rim and a lower-signal-intensity central zone on T2-weighted images. The central area of low signal intensity corresponds to the fibrocollagenous tissue seen in the core of the lesion at histologic analysis, and the surrounding area of high signal intensity corresponds to the presence of more myxomatous tissue (33). The target sign was first described in neurofibromas, although it can also be seen in schwannomas and malignant PNSTs.

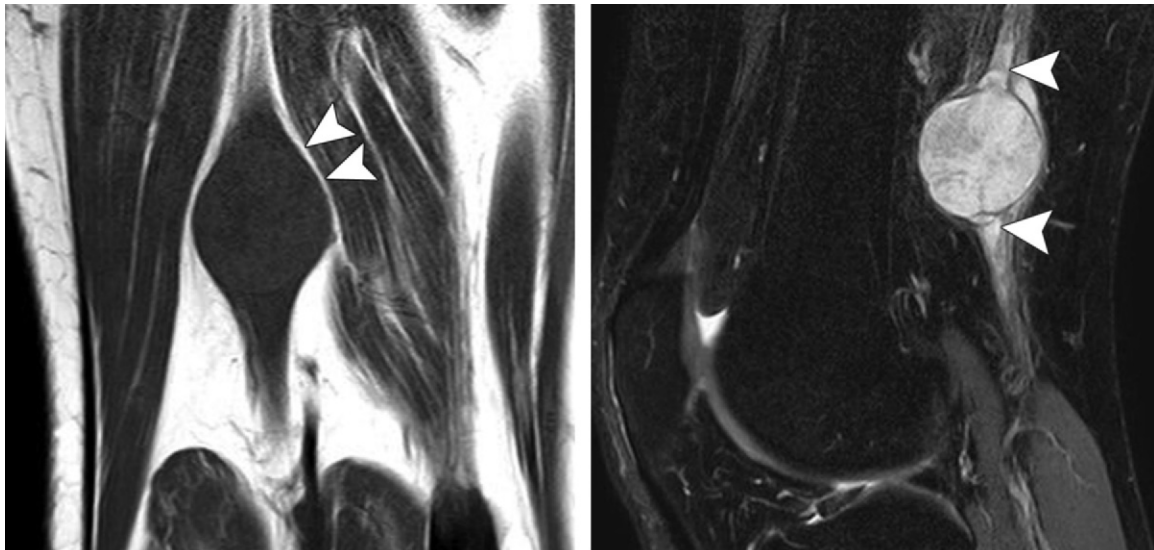


Figure 13. Neurofibroma in a 57-year-old patient with a known history of neurofibromatosis type 1. **(a)** Coronal T1-weighted MR image shows an ovoid low-signal-intensity mass in the posterior right thigh. Note the peripheral rim of fat (split fat sign) (arrowheads), a finding that indicates the intermuscular location of the mass. **(b)** Sagittal fat-suppressed T2-weighted MR image shows the common peroneal nerve (arrowheads) entering and exiting the mass (string sign).

Some authors believe that the MR imaging target sign always suggests a neurogenic neoplasm (32).

After contrast administration, the pattern of enhancement in PNSTs is variable and is commonly either heterogeneous and diffuse or peripheral. However, lesions demonstrating the target sign typically enhance more prominently at the center (33), with a surrounding area of nonenhancing myxoid tissue, effectively reversing the target sign.

Vascular Lesions (Hemangiomas and Vascular Malformations)

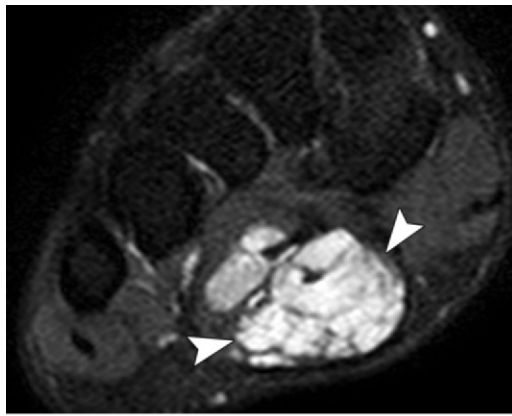
Among the classification systems for vascular lesions, the system developed by Mulliken and Glowacki (24) is the most widely accepted. Their system divides these lesions into two distinct groups: hemangiomas and vascular malformations. The former are considered true neoplastic lesions, whereas the latter are errors of vascular morphogenesis (6). There are other classification systems based on hemodynamic characteristics (34) at dynamic time-resolved contrast-enhanced MR angiography that divide vascular malformations into slow-flow malformations (capillary, venous, lymphatic, capillary-venous, and capillary-

lymphatic-venous malformations) and high-flow malformations (arteriovenous fistulas, arteriovenous malformations).

Hemangiomas and low-flow vascular malformations (eg, venous malformations) may manifest as soft-tissue masses in the extremities with a cystic appearance at MR imaging, sometimes in an intramuscular location (Fig 14). They are usually hypo- or isointense on T1-weighted images and hyperintense on T2-weighted images. Prominent vessels are usually seen within and around these lesions. In cases of hemorrhage or thrombosis, heterogeneous signal intensity can be observed on T1-weighted images (35). High proteinaceous or hemorrhagic content may cause internal fluid-fluid levels (36). Foci of signal void (representing high-flow vascular channels, phleboliths, or thrombi) may be interspersed with areas of increased signal intensity (representing fatty septa) (37). Avid enhancement after gadolinium administration is usually seen, a finding that reflects the vascular nature of these lesions.

Glomus Tumors

Glomus tumors represent a distinct entity. They occur as small tumors of the digits in patients between 30 and 50 years of age, with no gender



a.



b.

Figure 14. Hemangioma in the plantar aspect of the right foot in a 17-year-old patient. **(a)** Axial fat-suppressed T2-weighted MR image depicts a lobulated, hyperintense intramuscular mass with numerous septa (arrowheads) within the flexor digitorum brevis muscle. **(b)** On a coronal gadolinium-enhanced fat-suppressed T1-weighted MR image, the mass demonstrates intense lobular enhancement. Spared fat foci between the lobular vascular channels are also depicted.

predilection. Glomus tumors are rare benign neoplasms (hamartomas) that arise from a neuroarterial structure called the glomus body, are highly concentrated in the digits, and account for 1%–4.5% of tumors in the hand. MR imaging features that are considered diagnostic for glomus tumor include intermediate or low signal intensity on T1-weighted images, marked hyperintensity on T2-weighted images (Fig 15), and strong enhancement on postcontrast images (16).

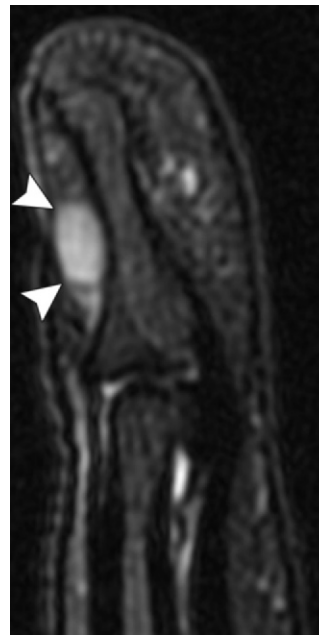


Figure 15. Glomus tumor in a 41-year-old woman with a history of a mass in the dorsal aspect of the right third finger. Sagittal fat-suppressed T2-weighted MR image shows a small, well-defined, rounded high-signal-intensity lesion (arrowheads) in the typical location of a glomus tumor (dorsum of the distal phalanx).

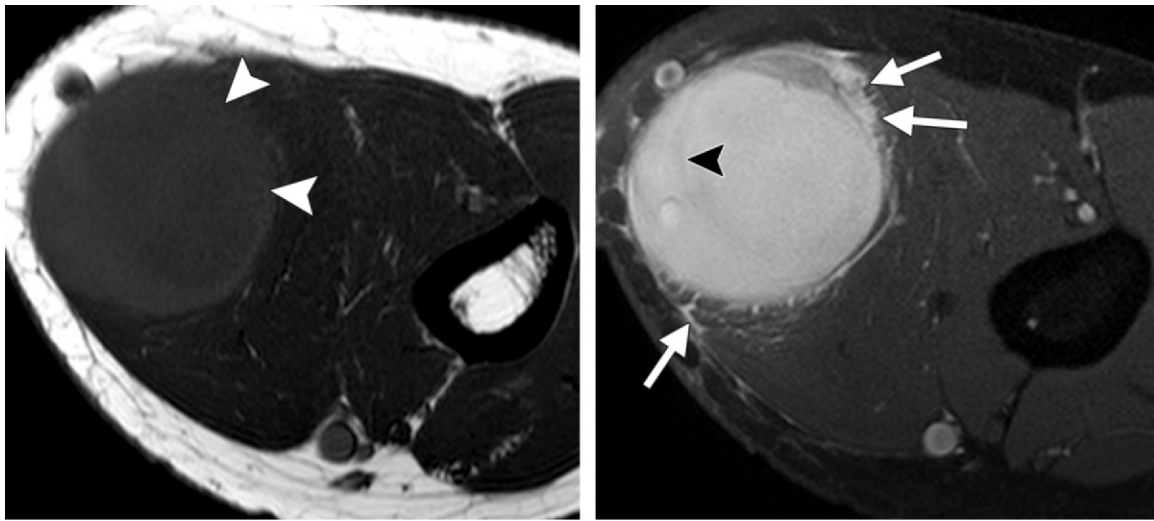
Malignant (and Intermediate-Grade) Solid Lesions

We have categorized the remaining (malignant) tumors according to the WHO classification system established in 2002 (4) and in descending order of frequency. Extraskeletal myxoid chondrosarcomas and synovial sarcomas (discussed later) are considered tumors of uncertain differentiation.

Undifferentiated Pleomorphic Sarcoma

UPS comprises a group of tumors formerly known as malignant fibrous histiocytoma and represents the most frequently seen soft-tissue sarcoma (deep seated or intramuscular) in adults over 50 years of age (38). Most of these tumors involve the extremities, the lower limbs being the most common site of involvement (up to 50% of cases) (38,39).

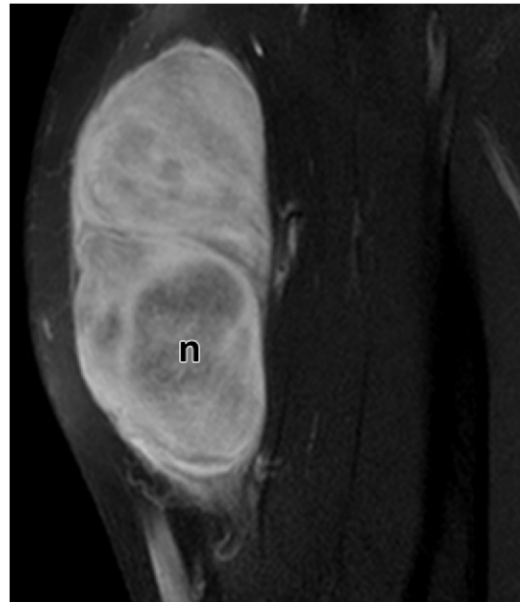
UPS are tumors with no specific light microscopic features apart from collagen production and therefore represent a diagnosis of exclusion. These tumors manifest as painless, circumscribed, lobulated masses with necrotic and cystic degeneration or hemorrhage. Calcification or ossification within the tumor may be seen in up to 5%–20% of cases. Bone erosion or infiltration is common (40). The signal intensity of UPS at MR imaging is nonspecific and depends on the cellularity and the myxoid content of the lesion as well as the presence of hemorrhage, necrosis, and calcification (40).



a.

b.

Figure 16. UPS in a 62-year-old man. **(a)** Axial T1-weighted MR image of the left upper arm shows a circumscribed intermediate-signal-intensity mass (arrowheads) within the biceps brachii muscle. **(b)** On an axial T2-weighted MR image, the mass demonstrates homogeneous increased signal intensity, with thin internal septa (arrowhead) and perilesional edema (arrows). **(c)** Sagittal gadolinium-enhanced fat-suppressed T1-weighted MR image shows the mass with diffuse enhancement and an area of relative nonenhancement inferiorly, likely due to a necrotic center (*n*).



c.

These tumors usually have low to intermediate signal intensity on T1-weighted images and intermediate to high signal intensity on T2-weighted images. Postcontrast enhancement is often more pronounced at the tumor periphery than at the center because of the central location of hemorrhage, necrosis, and myxoid components (Figs 16, 17) (41).

Myxoid Sarcomas

Myxofibrosarcoma.—Myxofibrosarcoma is among the most common sarcomas in elderly patients, manifesting as superficial soft-tissue masses in the lower limbs. It was formerly known as myxoid malignant fibrous histiocytoma (42).

Histologically, myxofibrosarcoma resembles myxoid liposarcoma, demonstrating multinodular growth and a myxoid stroma (40). Myxofibrosarcomas often have low to intermediate signal intensity on T1-weighted images and high signal intensity on T2-weighted images with low-signal-intensity septa (Fig 18). The solid and myxomatous components have high signal intensity on T2-weighted MR images, with the myxoid compo-

nent demonstrating higher signal intensity similar to that of fluid (43). T2-weighted imaging findings reflect the myxoid content of low- and intermediate-grade myxofibrosarcoma, which is inversely proportional to tumor cellularity and grade. In a report from the Armed Forces Institute of Pathology, the authors recommend that the term *myxoid variant of malignant fibrous histiocytoma* be restricted to tumors in which one-half or more areas are myxoid (44). High-grade myxofibrosarcoma is not easily distinguished from other adult pleomorphic sarcomas at MR imaging (45).

At MR imaging and CT, low-grade myxofibrosarcoma may closely resemble other myxoid tumors, such as myxoma and myxoid liposarcoma

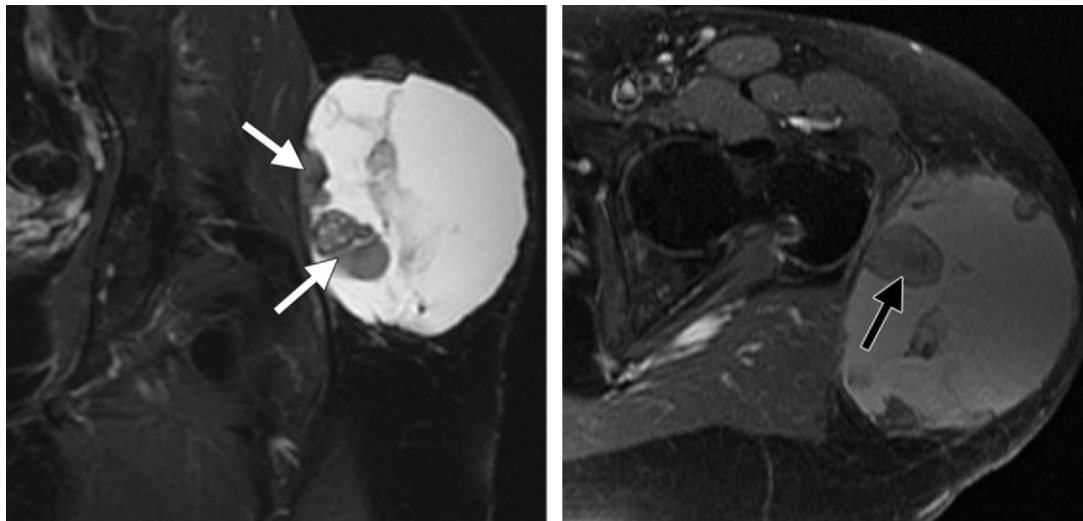


Figure 17. Bleeding within a UPS in a 58-year-old woman with a palpable mass in the left hip. **(a)** Coronal STIR MR image shows a high-signal-intensity mass within the lateral subcutaneous tissues. Note the presence of internal septa and nodular low-signal-intensity areas (arrows). **(b)** Axial gadolinium-enhanced fat-suppressed T1-weighted MR image depicts enhanced internal nodules (arrow). The high-signal-intensity content of the mass was similar on precontrast fat-suppressed T1-weighted images and likely represents subacute blood.

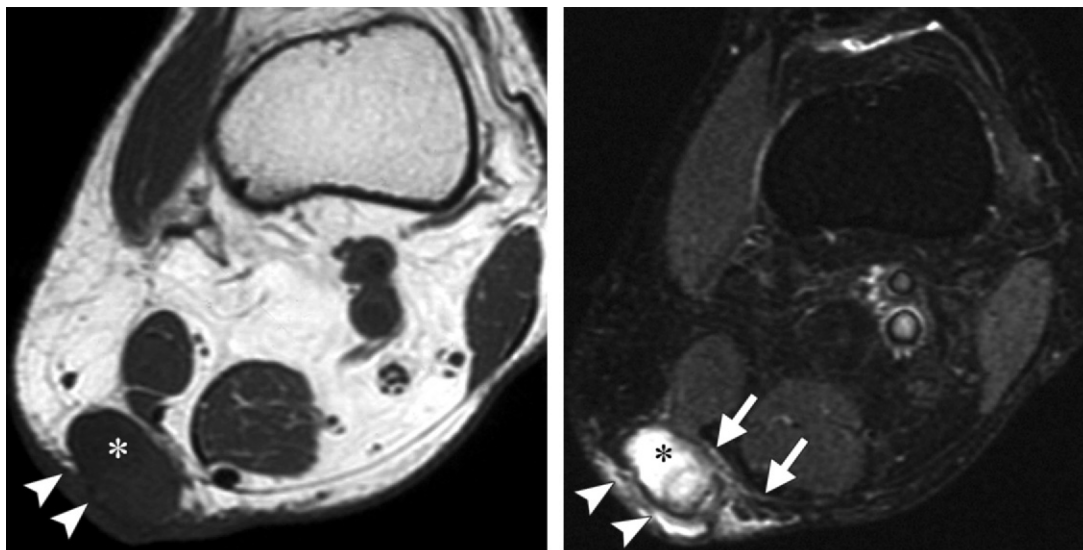


Figure 18. High-grade myxofibrosarcoma in a 74-year-old man. **(a)** Axial T1-weighted MR image shows a low-signal-intensity subcutaneous mass in the right posterior thigh (*). Diffuse spreading is noted along the epidermis (arrowheads). **(b)** On an axial fat-suppressed T2-weighted MR image, the mass (*) demonstrates an infiltrative growth pattern, with diffuse spreading along the subcutaneous fat, epidermis (arrowheads), and fascial planes (arrows).

Teaching Point

(43); however, fat is not present in myxofibrosarcomas, allowing their differentiation from myxoid liposarcomas (40). Postcontrast heterogeneous nodular and peripheral enhancement is often seen in the solid components (43).

In a series of 21 patients by Kaya et al (46), myxofibrosarcoma demonstrated a predominant

infiltrative growth pattern extending along fascial planes (with T2 hyperintensity) and a focal growth pattern surrounded by adipose tissue (although histologically infiltrative), both with myxoid foci

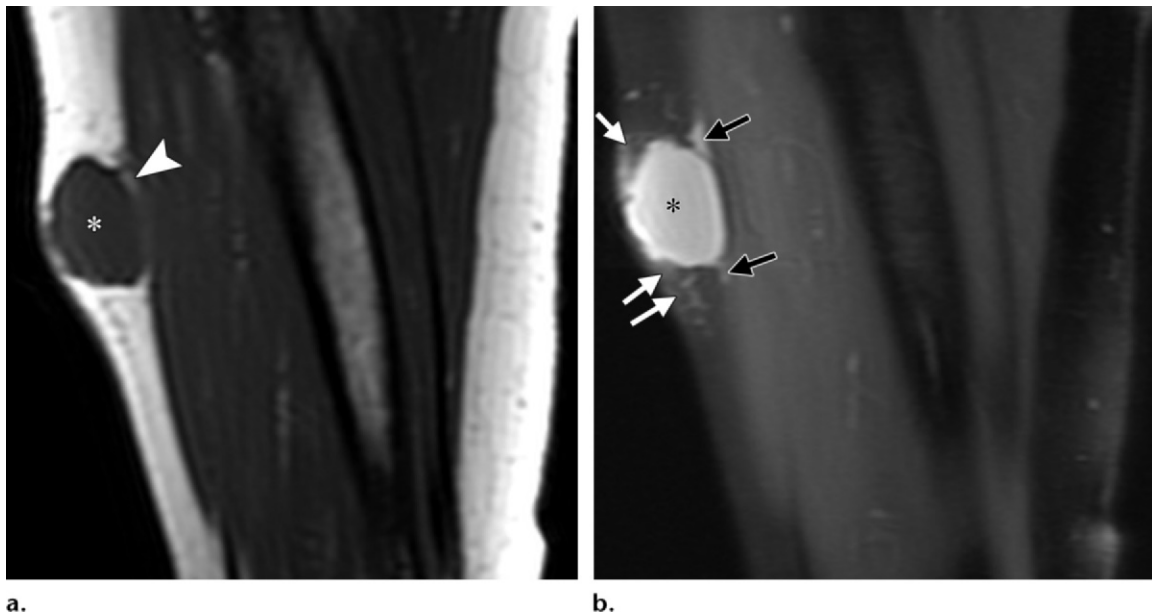


Figure 19. High-grade myxofibrosarcoma in a 66-year-old woman. **(a)** Sagittal T1-weighted MR image shows an ovoid mass (*) within the anterior subcutaneous tissues of the left upper arm. The mass has only a partial fat rim posteriorly (arrowhead). **(b)** On a sagittal fat-suppressed T2-weighted MR image, the mass (*) demonstrates homogeneous increased signal intensity. Note the irregular margins, increased perifascial signal intensity (black arrows), and high signal intensity within the dermal layer (white arrows). Diffuse enhancement was seen on contrast-enhanced fat-suppressed T1-weighted images.

(Figs 18, 19). This unusual characteristic of extending along fascial planes beyond the epicenter of the primary tumor is believed to account at least partially for the propensity of myxofibrosarcoma for multiple recurrences. A local recurrence rate of 55%–63% has been described. This recurrence appears to be independent of histologic grade and depth of tumor invasion. Myxofibrosarcomas tend to become progressively higher in grade at recurrence. An infiltrative pattern of recurrence and distant metastases to the lungs, pleura, bone, adrenal glands, soft tissue, and mesentery have been described even in low-grade myxofibrosarcoma (43).

Myxoid Liposarcoma.—Myxoid liposarcomas represent the second most common subtype of liposarcoma after well-differentiated liposarcomas (39). They occur mainly in the intermuscular fascial planes or deep-seated areas in the lower extremity, particularly the thigh, in young adults.

Myxoid liposarcoma has an intermediate prognosis. It often recurs and metastasizes to unusual locations such as the retroperitoneum and the opposite extremity, even before spreading to the lungs (40).

At histologic examination, myxoid liposarcomas consist of a plexiform vascular network, a mixture of stellate and spindle-shaped mesenchy-

mal cells, and lipoblasts set against a basophilic myxoid ground substance that often contains microcystic areas (47). Because the fat content is often less than 10%–25% of the tumor volume, MR imaging may not depict the typical features of a lipomatous tumor (48,49). The presence of a large component of myxoid matrix is the cause of the homogeneous, very long relaxation times mimicking a cystic lesion on T1- and T2-weighted images (47).

Myxoid liposarcoma with a cystic appearance at MR imaging has a reported prevalence of up to 22% (47,49). However, in a series by Mi-Sook et al (49), up to 78% of cases exhibited lacy or linear and amorphous foci representing fat, with high signal intensity on T1-weighted images (Fig 20a) and intermediate signal intensity on T2-weighted images (Fig 20b). After contrast administration, these tumors may show (a) homogeneous (total) or heterogeneous (partial) enhancement patterns, or (b) no enhancement at all (49), in which case US may be a useful tool. A pattern of gradually increasing enhancement over time has been described (49,50).

Myxoid liposarcoma with a large myxoid component is the lesion most commonly confused with intramuscular myxoma (30). However, its typical intermuscular location (28) and the presence of internal foci of high signal intensity on T1-weighted images help distinguish it from intramuscular myxoma. Furthermore, the

Teaching
Point



Figure 20. Myxoid liposarcoma in a 74-year-old man with a history of an enlarging mass in the right popliteal fossa. **(a)** Sagittal T1-weighted MR image shows high-signal-intensity foci of fat (arrowhead) within a predominantly low-signal-intensity mass (arrows). **(b)** On a sagittal fat-suppressed T2-weighted MR image, the mass demonstrates high signal intensity and contains fatty septa (black arrowheads) and a fatty nodule (white arrowhead), both of which appear hypointense. **(c)** On a sagittal gadolinium-enhanced T1-weighted MR image, the mass (arrows) demonstrates heterogeneous enhancement. Note the deviation of the course of the popliteal artery (*p*).

enhancement patterns of these two entities are different.

Extraskeletal Myxoid Chondrosarcoma.—Myxoid chondrosarcomas are multinodular tumors with abundant myxoid matrix and malignant chondroblast-like cells. There is no evidence of cartilaginous differentiation. The main sites of involvement are the deep soft tissues of the proximal extremities, most commonly in patients aged 50–60 years (51). These tumors usually appear as lobulated soft-tissue masses that are generally ill defined and heterogeneous (due to necrosis and hemorrhage) (40); however, well-delimited and homogeneous variants have also been described.

At MR imaging, their signal intensity is variable, especially on T1-weighted images (hyperintense foci due to hemorrhage may be present). On T2-weighted images, myxoid chondrosarcomas are usually hyperintense due to their myxoid content. In a series of 19 patients, Tateishi et al (51) described multilobular soft-tissue masses often invading extracompartmental, bony, and vascular structures, with fibrous septa and peripheral, diffuse, or mixed enhancement patterns. Contrast-enhanced images may also show rings and arcs, reflecting the lobulated growth pattern of cartilaginous tumors (49).

Synovial Sarcoma

Synovial sarcoma is a relatively common soft-tissue malignancy, accounting for approximately 5% of primary soft-tissue sarcomas in a large series from the Armed Forces Institute of Pathology

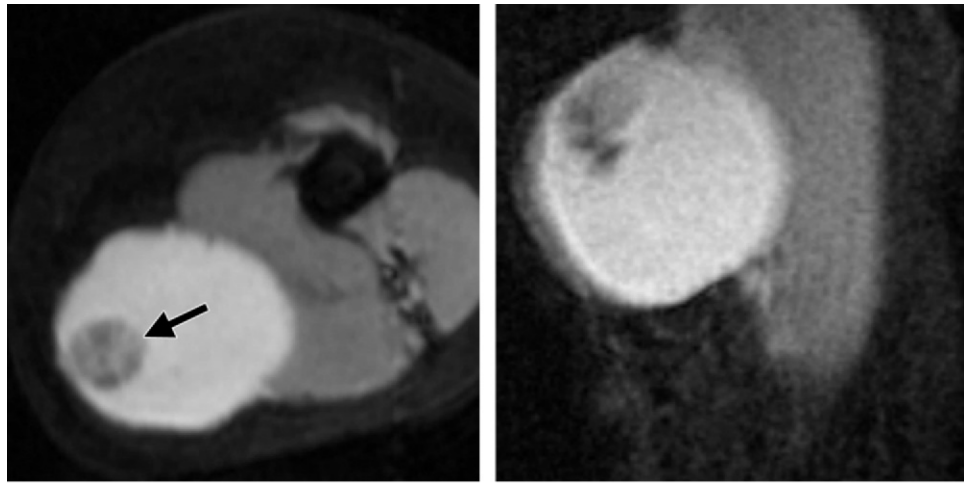


Figure 21. Synovial sarcoma in an unusual (superficial) location in a 40-year-old woman. **(a)** Axial fat-suppressed T2-weighted MR image of the right upper arm shows a large ovoid mass within the anterior subcutaneous tissues. The mass demonstrates increased signal intensity with a low-signal-intensity (calcified) internal nodule (arrow). Note its ill-defined borders, a finding that suggests invasion of the underlying musculature. **(b)** On a sagittal contrast-enhanced fat-suppressed T1-weighted MR image, the mass demonstrates diffuse heterogeneous enhancement.

(39). It most commonly affects the extremities in adolescents and young adults, often near joints (particularly the popliteal fossa) (52).

Despite its name, synovial sarcoma does not arise from synovium but from mesenchymal tissue and is named for its histologic resemblance to synovium. The name is, in fact, a misnomer, since it is related to the appearance of cells rather than their origin (53). There are three main histologic subtypes of synovial sarcoma: *(a)* a classic biphasic type comprising both spindle and epithelial cells; *(b)* a monophasic type, which usually demonstrates only a spindle cell component (53); and *(c)* the poorly differentiated type, which is generally epithelioid with high mitotic activity and geographic necrosis (52). The current WHO classification system includes synovial sarcomas under “Tumors of Uncertain Differentiation,” which accounts for the rarity of intraarticular cases (4,53).

At MR imaging, multilobulation and marked heterogeneity (“triple signal intensity sign”) with hemorrhage, fluid levels, and septa (“bowl of grapes sign”) have been described (52). Over 40% of lesions demonstrate high signal intensity on both T1- and T2-weighted images, a finding that is consistent with hemorrhage. Fluid-fluid levels are present in almost one-fifth of cases, and 35% of cases demonstrate areas of hyper-

iso-, and hypointensity relative to fat on T2-weighted images (triple signal intensity sign). This appearance reflects a combination of cystic and solid elements with hemorrhage and fibrous tissue (53). However, small lesions (<5 cm at presentation) may have a predominantly homogeneous appearance on T2-weighted images (Fig 21), a finding that, together with slow growth and well-defined margins, simulates a less aggressive process (54).

Soft-Tissue Metastases

Soft-tissue metastases (either subcutaneous or intramuscular) are very rare (55,56) and are often related to widespread disease or located near the site of a primary tumor. Their manifestation is similar to that of soft-tissue sarcomas, although on occasion, well-defined, relatively homogeneous T2-hyperintense lesions are depicted. Metastases to muscle often show large areas of surrounding edema (55).

Conclusion

If a cystic-appearing lesion does not demonstrate totally homogeneous low signal intensity on T1-weighted images and homogeneous bright signal intensity on T2-weighted images, intravenous contrast administration is necessary to rule out a solid lesion (Fig 22). Contrast-enhanced imaging is also necessary if ill-defined borders, a thick rim, or thick internal septa are present, or if the

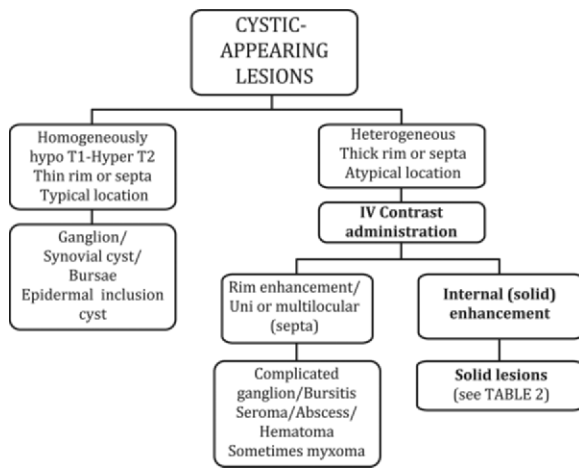


Figure 22. Flow chart illustrates the procedure for evaluating lesions with a cystic MR imaging appearance. Intravenous (IV) contrast administration can help distinguish between truly cystic (fluid-filled) lesions and solid lesions.

Table 2
Characteristic MR Imaging Features That May Help Identify Soft-Tissue Cystlike Solid Lesions

Type of Lesion	Morphology	T1 Signal Intensity	T2 Signal Intensity	Contrast Enhancement
Myxoma	Oval, fusiform (no string sign)	Surrounding fat rim	Possible perilesional edema	Peripheral with or without heterogeneous internal enhancement
PNST	Fusiform, string sign	Split fat sign	Target sign	Variable (generally intense, central in target sign lesions)
UPS	Circumscribed, lobulated	Low to intermediate, possible hyperintense foci	Central necrosis or hemorrhage, possible perilesional edema	Variable (often greater at the periphery)
Myxofibrosarcoma	Infiltrative or focal	Fat rim (focal type only)	Perifascial spread	Heterogeneous
Myxoid liposarcoma	Multinodular	Fat foci	Possible perilesional edema	Variable (gradual over time)
Extraskeletal myxoid chondrosarcoma	Well- or ill-defined	Variable, possible hyperintense foci	Heterogeneous, necrosis or hemorrhage	Variable
Synovial sarcoma	Multilobulated	Possible hyperintense foci (hemorrhage)	Heterogeneous (except for small lesions), triple signal intensity sign, bowl of grapes sign	Variable

lesion has an atypical location for either (a) a synovial-ganglion cyst or a bursa, or (b) a collection (in the proper clinical setting).

If partial or complete internal enhancement is present, biopsy (prior to excision) is indicated, with the options in small or superficial tumors including fine-needle aspiration biopsy, core biopsy, and excisional biopsy. Rim enhancement is usually characteristic of truly cystic lesions but may also be present in solid lesions such as myxoma, so that other features must

be taken into account (subtle internal enhancement, intramuscular location, peripheral fat rim, perilesional edema). Morphology (eg, fusiform-shaped PNSTs) and location (eg, extending along nerve roots [PNST], intramuscular location [myxoma]), along with certain characteristic MR imaging features, may help identify specific solid lesions (Tables 1, 2).

MR imaging is also useful in determining the exact location of a lesion, characterizing its relationship to neighboring structures (intramuscular or intraosseous tumor extent, neurovascular involvement, presence of regional lymph nodes), and guiding biopsy (accessing solid or enhancing components, avoiding necrotic areas, and taking the best path to avoid dissemination).

Acknowledgment.—The authors thank Luis Herráiz, MD, for his valuable help and advice in preparing the manuscript.

References

1. Wu JS, Hochman MG. Soft-tissue tumors and tumorlike lesions: a systematic imaging approach. *Radiology* 2009;253(2):297–316.
2. Ma LD, McCarthy EF, Bluemke DA, Frassica FJ. Differentiation of benign from malignant musculoskeletal lesions using MR imaging: pitfalls in MR evaluation of lesions with a cystic appearance. *AJR Am J Roentgenol* 1998;170(5):1251–1258.
3. Peterson KK, Renfrew DL, Feddersen RM, Buckwalter JA, el-Khoury GY. Magnetic resonance imaging of myxoid containing tumors. *Skeletal Radiol* 1991;20(4):245–250.
4. Fletcher CD, Unni KK, Mertens F, eds. WHO classification of tumours: pathology and genetics of tumours of soft tissue and bone. Lyon, France: IARC, 2002.
5. Johnstone AJ, Beggs I. Ultrasound imaging of soft-tissue masses in the extremities. *J Bone Joint Surg Br* 1994;76(5):688–689.
6. Navarro OM, Laffan EE, Ngan BY. Pediatric soft-tissue tumors and pseudotumors: MR imaging features with pathologic correlation. I. Imaging approach, pseudotumors, vascular lesions, and adipocytic tumors. *RadioGraphics* 2009;29(3):887–906.
7. Gold GE, Suh B, Sawyer-Glover A, Beaulieu C. Musculoskeletal MRI at 3.0 T: initial clinical experience. *AJR Am J Roentgenol* 2004;183(5):1479–1486.
8. Gielen JL, De Schepper AM, Parizel PM, Wang XL, Vanhoenacker F. Additional value of magnetic resonance with spin echo T1-weighted imaging with fat suppression in characterization of soft tissue tumors. *J Comput Assist Tomogr* 2003;27(3):434–441.
9. Helms CA. The use of fat suppression in gadolinium-enhanced MR imaging of the musculoskeletal system: a potential source of error. *AJR Am J Roentgenol* 1999;173(1):234–236.
10. Jelinek J, Kransdorf MJ. MR imaging of soft-tissue masses: mass-like lesions that simulate neoplasms. *Magn Reson Imaging Clin N Am* 1995;3(4):727–741.
11. Shapeero LG, Vanel D, Verstraete KL, Bloem JL. Fast magnetic resonance imaging with contrast for soft tissue sarcoma viability. *Clin Orthop Relat Res* 2002 (397):212–227.
12. Kransdorf MJ, Murphey MD. Radiologic evaluation of soft-tissue masses: a current perspective. *AJR Am J Roentgenol* 2000;175(3):575–587.
13. Harish S, Lee JC, Ahmad M, Saifuddin A. Soft tissue masses with “cyst-like” appearance on MR imaging: distinction of benign and malignant lesions. *Eur Radiol* 2006;16(12):2652–2660.
14. Verstraete KL, De Deene Y, Roels H, Dierick A, Uyttendaele D, Kunnen M. Benign and malignant musculoskeletal lesions: dynamic contrast-enhanced MR imaging—parametric “first-pass” images depict tissue vascularization and perfusion. *Radiology* 1994;192(3):835–843.
15. van der Woude HJ, Verstraete KL, Hogendoorn PC, Taminiau AH, Hermans J, Bloem JL. Musculoskeletal tumors: does fast dynamic contrast-enhanced subtraction MR imaging contribute to the characterization? *Radiology* 1998;208(3):821–828.
16. van Rijswijk CS, Geirnaerd MJ, Hogendoorn PC, et al. Soft-tissue tumors: value of static and dynamic gadopentetate dimeglumine-enhanced MR imaging in prediction of malignancy. *Radiology* 2004;233(2):493–502.
17. van Rijswijk CS, Kunz P, Hogendoorn PC, Taminiau AH, Doornbos J, Bloem JL. Diffusion-weighted MRI in the characterization of soft-tissue tumors. *J Magn Reson Imaging* 2002;15(3):302–307.
18. Janzen DL, Peterfy CG, Forbes JR, Tirman PF, Genant HK. Cystic lesions around the knee joint: MR imaging findings. *AJR Am J Roentgenol* 1994;163(1):155–161.
19. Kim JY, Jung SA, Sung MS, Park YH, Kang YK. Extra-articular soft tissue ganglion cyst around the knee: focus on the associated findings. *Eur Radiol* 2004;14(1):106–111.
20. Helms CA, Major NM, Anderson MW, Kaplan P, Dussault R. Tendons and muscle. In: Schmidt R, ed. *Musculoskeletal MRI*. 2nd ed. Philadelphia, Pa: Elsevier, 2009; 50–79.
21. Pathria MN, Boutin RD. Magnetic resonance imaging of muscle. In: Schulthess GK, ed. *Musculoskeletal diseases 2009-1012: diagnostic imaging*. Milan, Italy: Springer, 2009; 57–63.
22. Mellado JM, Bencardino JT. Morel-Lavallée lesion: review with emphasis on MR imaging. *Magn Reson Imaging Clin N Am* 2005;13(4):775–782.
23. Hong SH, Chung HW, Choi JY, Koh YH, Choi JA, Kang HS. MRI findings of subcutaneous epidermal cysts: emphasis on the presence of rupture. *AJR Am J Roentgenol* 2006;186(4):961–966.
24. Mulliken JB, Glowacki J. Hemangiomas and vascular malformations in infants and children: a classification based on endothelial characteristics. *Plast Reconstr Surg* 1982;69(3):412–422.
25. Ly JQ, Gilbert BC, Davis SW, Beall DP, Richardson RR. Lymphangioma of the foot. *AJR Am J Roentgenol* 2005;184(1):205–206.

26. García-Alvarez F, Torcal J, Salinas JC, et al. Musculoskeletal hydatid disease: a report of 13 cases. *Acta Orthop Scand* 2002;73(2):227–231.
27. Merkle EM, Schulte M, Vogel J, et al. Musculoskeletal involvement in cystic echinococcosis: report of eight cases and review of the literature. *AJR Am J Roentgenol* 1997;168(6):1531–1534.
28. Murphey MD, McRae GA, Fanburg-Smith JC, Temple HT, Levine AM, Abouafia AJ. Imaging of soft-tissue myxoma with emphasis on CT and MR and comparison of radiologic and pathologic findings. *Radiology* 2002;225(1):215–224.
29. Bancroft LW, Kransdorf MJ, Menke DM, O'Connor MI, Foster WC. Intramuscular myxoma: characteristic MR imaging features. *AJR Am J Roentgenol* 2002;178(5):1255–1259.
30. Luna A, Martinez S, Bossen E. Magnetic resonance imaging of intramuscular myxoma with histological comparison and a review of the literature. *Skeletal Radiol* 2005;34(1):19–28.
31. Kransdorf MJ. Benign soft-tissue tumors in a large referral population: distribution of specific diagnoses by age, sex, and location. *AJR Am J Roentgenol* 1995;164(2):395–402.
32. Murphey MD, Smith WS, Smith SE, Kransdorf MJ, Temple HT. Imaging of musculoskeletal neurogenic tumors: radiologic-pathologic correlation. *RadioGraphics* 1999;19(5):1253–1280.
33. Banks KP. The target sign: extremity. *Radiology* 2005;234(3):899–900.
34. Jackson IT, Carreño R, Potparic Z, Hussain K. Hemangiomas, vascular malformations, and lymphovenous malformations: classification and methods of treatment. *Plast Reconstr Surg* 1993;91(7):1216–1230.
35. Dubois J, Soulez G, Oliva VL, Berthiaume MJ, Lapierre C, Therasse E. Soft-tissue venous malformations in adult patients: imaging and therapeutic issues. *RadioGraphics* 2001;21(6):1519–1531.
36. Hyodoh H, Hori M, Akiba H, Tamakawa M, Hyodoh K, Hareyama M. Peripheral vascular malformations: imaging, treatment approaches, and therapeutic issues. *RadioGraphics* 2005;25(suppl 1):S159–S171.
37. O'Connor EE, Dixon LB, Peabody T, Stacy GS. MRI of cystic and soft-tissue masses of the shoulder joint. *AJR Am J Roentgenol* 2004;183(1):39–47.
38. Murphey MD, Gross TM, Rosenthal HG. Musculoskeletal malignant fibrous histiocytoma: radiologic-pathologic correlation. *RadioGraphics* 1994;14(4):807–826.
39. Kransdorf MJ. Malignant soft-tissue tumors in a large referral population: distribution of diagnoses by age, sex, and location. *AJR Am J Roentgenol* 1995;164(1):129–134.
40. van Vliet M, Kliffen M, Krestin GP, van Dijke CF. Soft tissue sarcomas at a glance: clinical, histological, and MR imaging features of malignant extremity soft tissue tumors. *Eur Radiol* 2009;19(6):1499–1511.
41. Munk PL, Sallomi DF, Janzen DL, et al. Malignant fibrous histiocytoma of soft tissue imaging with emphasis on MRI. *J Comput Assist Tomogr* 1998;22(5):819–826.
42. Vilanova JC, Woertler K, Narváez JA, et al. Soft-tissue tumors update: MR imaging features according to the WHO classification. *Eur Radiol* 2007;17(1):125–138.
43. Waters B, Panicek DM, Lefkowitz RA, et al. Low-grade myxofibrosarcoma: CT and MRI patterns in recurrent disease. *AJR Am J Roentgenol* 2007;188(2):W193–W198.
44. Weiss SW, Enzinger FM. Myxoid variant of malignant fibrous histiocytoma. *Cancer* 1977;39(4):1672–1685.
45. De Schepper AM, Vandevenne JE. Tumors of connective tissue. In: de Schepper AM, Parizel PM, eds. *Imaging of soft tissue tumors*. 2nd ed. Berlin, Germany: Springer, 2001; 167–202.
46. Kaya M, Wada T, Nagoya S, et al. MRI and histological evaluation of the infiltrative growth pattern of myxofibrosarcoma. *Skeletal Radiol* 2008;37(12):1085–1090.
47. Jelinek JS, Kransdorf MJ, Shmookler BM, Abouafia AJ, Malawer MM. Liposarcoma of the extremities: MR and CT findings in the histologic subtypes. *Radiology* 1993;186(2):455–459.
48. Sundaram M, Baran G, Merenda G, McDonald DJ. Myxoid liposarcoma: magnetic resonance imaging appearances with clinical and histological correlation. *Skeletal Radiol* 1990;19(5):359–362.
49. Sung MS, Kang HS, Suh JS, et al. Myxoid liposarcoma: appearance at MR imaging with histologic correlation. *RadioGraphics* 2000;20(4):1007–1019.
50. Kim T, Murakami T, Oi H, et al. CT and MR imaging of abdominal liposarcoma. *AJR Am J Roentgenol* 1996;166(4):829–833.
51. Tateishi U, Hasegawa T, Nojima T, Takegami T, Arai Y. MRI features of extraskeletal myxoid chondrosarcoma. *Skeletal Radiol* 2006;35(1):27–33.
52. Murphey MD, Gibson MS, Jennings BT, Crespo-Rodriguez AM, Fanburg-Smith J, Gajewski DA. Imaging of synovial sarcoma with radiologic-pathologic correlation. *RadioGraphics* 2006;26(5):1543–1565.
53. O'Sullivan PJ, Harris AC, Munk PL. Radiological features of synovial cell sarcoma. *Br J Radiol* 2008;81(964):346–356.
54. Blacksin MF, Siegel JR, Benevenia J, Aisner SC. Synovial sarcoma: frequency of nonaggressive MR characteristics. *J Comput Assist Tomogr* 1997;21(5):785–789.
55. Abed R, Grimer RJ, Carter SR, Tillman RM, Abudu A, Jeys L. Soft-tissue metastases: their presentation and origin. *J Bone Joint Surg Br* 2009;91(8):1083–1085.
56. Beaman FD, Kransdorf MJ, Andrews TR, Murphey MD, Arcara LK, Keeling JH. Superficial soft-tissue masses: analysis, diagnosis, and differential considerations. *RadioGraphics* 2007;27(2):509–523.

MR Imaging in the Evaluation of Cystic-appearing Soft-Tissue Masses of the Extremities

Ana Bermejo, MD • Teresa Díaz De Bustamante, MD • Alberto Martínez, MD Roberto Carrera, MD • Elena Zabía, MD • Palmira Manjón, MD

RadioGraphics 2013; 33:833–855 • Published online 10.1148/rg.333115062 • Content Codes:   

Page 834

Besides truly cystic lesions such as ganglia or bursae, there are some solid masses that can also appear to be very T2 hyperintense. These lesions have been described as “cystlike” lesions by some authors.

Page 836

Evaluation with contrast material enhancement is indicated when a cystic-appearing lesion (*a*) is identified in an atypical location, or (*b*) has heterogeneous internal signal, a thick wall, multiple or thick septa, or solid components, findings that suggest that the lesion is not a simple cyst.

Page 844

Intramuscular myxoma must also be differentiated from other deep myxoid lesions located in the extremities, including myxoid PNSTs, myxofibrosarcoma, myxoid liposarcoma, extraskeletal myxoid chondrosarcoma, and UPS.

Pages 849

Fat is not present in myxofibrosarcomas, allowing their differentiation from myxoid liposarcomas. Post-contrast heterogeneous nodular and peripheral enhancement is often seen in the solid components.

Pages 850

Myxoid liposarcoma with a large myxoid component is the lesion most commonly confused with intramuscular myxoma. However, its typical intermuscular location and the presence of internal foci of high signal intensity on T1-weighted images help distinguish it from intramuscular myxoma.